



HAL
open science

Neutral Lipopolyplexes for In Vivo Delivery of Conventional and Replicative RNA Vaccine

Federico Perche, Rudy Clemençon, Kai Schulze, Thomas Ebensen, Carlos Guzman, Chantal Pichon

► **To cite this version:**

Federico Perche, Rudy Clemençon, Kai Schulze, Thomas Ebensen, Carlos Guzman, et al.. Neutral Lipopolyplexes for In Vivo Delivery of Conventional and Replicative RNA Vaccine. *Molecular Therapy - Nucleic Acids*, 2019, 17, pp.767-775. 10.1016/j.omtn.2019.07.014 . hal-02321815

HAL Id: hal-02321815

<https://hal.science/hal-02321815v1>

Submitted on 23 Nov 2020

HAL is a multi-disciplinary open access archive for the deposit and dissemination of scientific research documents, whether they are published or not. The documents may come from teaching and research institutions in France or abroad, or from public or private research centers.

L'archive ouverte pluridisciplinaire **HAL**, est destinée au dépôt et à la diffusion de documents scientifiques de niveau recherche, publiés ou non, émanant des établissements d'enseignement et de recherche français ou étrangers, des laboratoires publics ou privés.

Neutral Lipopolyplexes for *In Vivo* Delivery of Conventional and Replicative RNA Vaccine

Federico Perche,¹ Rudy Clemençon,¹ Kai Schulze,² Thomas Ebensen,² Carlos A. Guzmán,² and Chantal Pichon¹

¹Centre de Biophysique Moléculaire, UPR4301 CNRS Rue Charles Sadron Orléans, Orléans Cedex 02, France; ²Department of Vaccinology and Applied Microbiology, Helmholtz Centre for Infection Research, 38124 Braunschweig, Germany

Nucleic acid vaccination relies on injecting DNA or RNA coding antigen(s) to induce a protective immune response. RNA vaccination is being increasingly used in preclinical and clinical studies. However, few delivery systems have been reported for *in vivo* delivery of RNA of different sizes. Using a tripartite formulation with RNA, cationic polymer, and anionic liposomes, we were able to encapsulate RNA into neutral lipopolyplexes (LPPs). LPPs were stable *in vitro* and successfully delivered conventional RNA and replicative RNA to dendritic cells *in cellulo*. Their injection led to reporter gene expression in mice. Finally, administration of LPP-Replicon RNA (RepRNA) led to an adaptive immune response against the antigen coded by the RepRNA. Accordingly, LPPs may represent a universal formulation for RNA delivery.

INTRODUCTION

RNA vaccination is an expanding field with applications from cancer immunotherapy, infectious diseases, tissue regeneration and protein replacement therapy.^{1–3} Contrary to DNA, RNA does not need to cross the nuclear envelope for expression, a feature that results in higher transfection efficiency over DNA of differentiated or non-dividing cells such as neurons^{4–6} or dendritic cells.⁷ However, nuclease degradation and inefficient or short-time expression of RNA still limits its application.^{1,8} While local intranodal injection of RNA results in effective induction of a specific immune response,^{9–11} intramuscular (i.m.), subcutaneous, or intravenous (i.v.) injections would be preferred for large-scale preventive vaccination. For that, different types of nanoparticles, from micelles to lipidic nanoparticle RNA-encoded antigens, need to be presented to lymphocytes by dendritic cells (DCs) to induce an immune response against cancer or viruses.^{1,12} Liposome- or lipidic nanoparticle-mediated delivery of RNA encoding cancer or viral antigens resulted in protective immune responses in several models (mice and Macaque) and in humans.^{1,7,13–23} Among the strategies aimed at inducing antigenic presentation by antigen-presenting cells, systemic delivery of RNA to splenic DCs reached clinical trials.^{16,24} Kranz et al.¹⁶ used negatively-charged unPEGylated lipopolyplexes without ligand, which selectively accumulate in the spleen to transfect splenic DCs and induce a protective immune response against melanoma. Our group has developed ternary complexes comprising a cationic polymer and mannoseylated liposomes, designated lipopolyplexes (LPPs), for mRNA delivery to splenic DCs.²⁵ We previously demonstrated that mRNA LPPs show superior immunogenicity and effec-

tiveness in controlling tumor growth over mRNA lipopolyplexes and mRNA polyplexes.^{15,26} The first generation of mannoseylated LPPs were formed with the PEGylated histidylated polylysine (PEG-HpK) cationic polymer and lipophosphoramidate liposomes made with N-methyl imidazolium lipophosphoramidate (cationic lipid), histamine lipophosphoramidate (protonable lipid), and a mannoseylated lipid to favor endocytosis by DCs.⁷ The second generation of mannoseylated LPPs were also formed with the PEG-HpK polymer and lipophosphoramidate liposomes but included a glycolipid containing a tri-antenna of α -D-mannopyranoside instead of a monovalent mannose for improved endocytosis by DCs.²⁷ Cationic and mannoseylated LPPs exerted powerful anti-tumor effects when used as therapeutic vaccine in different experimental tumor models.^{14,15}

In addition to complexing conventional mRNA into stable nanoparticles, a further improvement in RNA vaccination could be gained by the use of self-amplifying RNA or Replicon RNA (RepRNA), particularly for RNA vaccines against influenza.^{28,29} Auto-amplifying RepRNA is generated from a viral genome, a positive-RNA strand that bears the ability to replicate and translate without generating infectious progeny because it lacks at least one structural gene.^{30,31} Compared with mRNA, RepRNA allows amplification of RNA copies in the cytoplasm of host cells, which offer several rounds of antigen production.^{32–35} As there are no DNA intermediates, there is no risk of integration. Injection of RepRNA extends the duration and magnitude of antigen expression compared to mRNA, giving equivalent protection against influenza at lower doses than mRNA.^{3,26,36,37} Since RepRNA based-vaccination is a more recent strategy than vaccination with mRNA, there are few formulations developed for their delivery.^{1,3,28}

In this study, we evaluated the capability of neutrally charged LPPs, including a mannoseylated lipid, to transfect DCs.^{7,14,15} We determined the physico-chemical properties of LPPs and their efficiency

Received 19 February 2019; accepted 17 July 2019;
<https://doi.org/10.1016/j.omtn.2019.07.014>

Correspondence: Federico Perche, Centre de Biophysique Moléculaire, UPR4301 CNRS Rue Charles Sadron Orléans, Orléans Cedex 02, France.

E-mail: federico.perche@cnrs-orleans.fr

Correspondence: Chantal Pichon, Centre de Biophysique Moléculaire, UPR4301 CNRS Rue Charles Sadron Orléans, Orléans Cedex 02, France.

E-mail: chantal.pichon@cnrs.fr



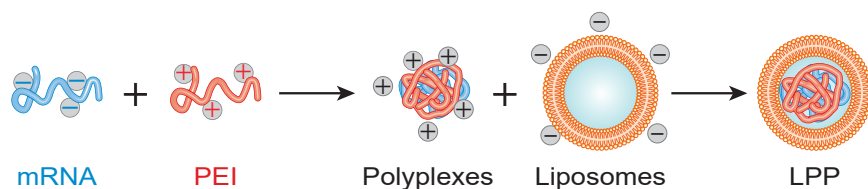


Figure 1. Formation of LPPs

to transfect DCs both *in vitro* and *in vivo*. Administration of LPPs prepared with conventional RNA or self-replicative RNA resulted in reporter gene expression in mice and the induction of an antigen-specific immune response when LPPs were prepared with RNA encoding an influenza antigen.

RESULTS AND DISCUSSION

Formation of Neutral RNA LPPs

A majority of previous studies reported the functionality upon *in vivo* injection of either positively-charged^{7,15,38} or negatively-charged^{16,39} RNA complexes. In this study, we chose to use a neutral formulation, as they are known to have benefits over the others. Since, neutral RNA lipoplexes are unstable,¹⁶ we used an LPP strategy to form neutral RNA complexes. We produced neutral nanoparticles that would benefit from their prolonged blood circulation compared to positively-charged and negatively-charged nanoparticles.^{40–44} Neutral nanoparticles show negligible protein adsorption and decreased complement activation compared to positive and negative ones.^{40,42,45} Combined with PEGylation of the liposomes, the neutral surface is expected to extend blood circulation and increase the chances of nanoparticle retention in the desired organs after *i.v.* injection.^{42,44,46} Neutral charge is also expected to favor the penetration of the extracellular matrix and distribution to lymphatics for enhanced delivery to lymph nodes after interstitial (*i.m.*) injection.^{47–49}

The formation of LPPs is described in Figure 1. LPPs consist in a tripartite mix of RNA, a polymer, and liposomes. To form LPPs without cationic lipids, we first complexed RNA with polyethylenimine (PEI), the most frequently used polymer in LPP formulations,^{50–52} before adding anionic liposomes. As shown in Table 1, polyplexes prepared at N/P ratios 4.5–9 had mean diameters of 150–170 nm. We selected an N/P ratio of 6, yielding complexes of 166 nm and +20 mV. For the anionic liposomes, we used monodisperse liposomes containing 5% 1,2-distearoyl-sn-glycero-3-phosphoethanolamine-N-[carboxy(polyethylene glycol)-2000] (DSPE-PEG) to provide stability in biological fluids,^{53,54} 40% molar negatively charged 1,2-dioleoyl-sn-glycero-3-phosphate (DOPA) to favor interaction with the positively charged polyplex and for immunogenicity,^{55,56} the fusogenic lipid 1,2-dioleoyl-sn-glycero-3-phosphoethanolamine (DOPE) to promote endosomal escape,⁵⁷ and a mannosylated lipid (16:0 1,2-dipalmitoyl-sn-glycero-3-phospho((ethyl-1',2',3'-triazole)triethyleneglycolmannose [PA-PEG3-mannose]) to engage the mannose receptor on dendritic cells.^{7,31} We fixed the total PEGylated lipid content at 10% (5% DSPE-PEG + 5% PEG-mannose) to decrease non-specific accumulation based on previous studies.^{54,58,59} In line with the results of Kranz

et al.¹⁶ on splenic DC transfection with RNA lipoplexes, 40% DOPE helper lipid was included. Liposomes were monodisperse with a diameter of 140–150 nm and a polydispersity index (PDI; measure of size distribution) below 0.2 (PDI 0.14/0.05) and a negative charge of –18/6 mV. Next, we determined the liposome/PEI ratio yielding neutral LPPs (Table 2). Entrapping the polyplexes increased the liposome diameter from 140 to 160–190 nm and decreased the size distribution, resulting in monodisperse LPPs (PDI 0.13–0.15), features observed previously.^{14,60,61} Moreover, formation of LPPs shielded the positive charges of polyplexes (+20 mV), resulting in neutrally charged LPPs (0.5–2.5 mV), supporting encapsulation of polyplexes in liposomes. Encapsulation was verified by electron microscopy (Figures 2B and 2D) and was in accordance with previous studies.^{60,62} A DOPA/PEI molar ratio of 23 was used for further studies. Note that complexes prepared with self-replicative RNA, which is larger than conventional mRNA (10,000 nt for VEE-GFP RNA versus 1,000 nt for GFP RNA), were also under 200 nm and neutral: 180/10 nm and 1/0.9 mV.

Systemic administration of RNA complexes requires avoiding aggregation or destruction of complexes in physiological fluids and protection from RNase degradation.¹ Protection against RNase degradation was checked by gel electrophoresis (Figure 2A). Whereas naked RNA was degraded by RNase (Figure 2A, lane 2), LPP formulation protected it from degradation (Figure 2A, lane 3).

We monitored the size of LPPs in serum and at 37°C by dynamic light scattering (Figure 2C). After 6 h incubation, there was no aggregation of LPPs, indicating its stability. Note that LPPs prepared with unPEGylated liposomes aggregated to $\approx 1 \mu\text{m}$ in 1 h, confirming PEG-mediated stabilization of the particles in serum as in Buysen et al.⁵⁹ and Zhao et al.⁶³

In Cellulo Transfection Activity

LPPs prepared with 25K PEI and anionic liposomes exhibited a low cytotoxicity (10%–15%) toward murine DCs, similar to that of the lipofectamine messenger max (LFM) control (Figure 3B). PEI 25K polyplexes were, however, toxic (>20% decrease in cell metabolism), in agreement with Wang et al.⁶⁰ Then, we checked the transfection efficiency with conventional mRNA. Although lipofectamine showed superior transfection efficiency over LPPs at 4 h and 24 h (25% transfected cells versus 2.5% at 4 h and 43% versus 22% at 24 h), transfection efficiency was similar at 48 h post-transfection (27% and 22%, respectively), suggesting differences in expression kinetics due to composition and structure differences in the two kinds of RNA complexes (Figure 3A).^{39,64,65}

Transfection of murine DCs with LPPs prepared with GFP RepRNA resulted in 14%–16% transfected cells through 24 h to 72 h

Table 1. Size and Zeta Potential of Polyplexes

PEI/RNA (N/P Ratio)	Size (nm)	Zeta Potential (mV)
4.5	172/42	-2/5
6	166/10	20/9
7.5	165/8	13/2
9	156/9	10/3

post-transfection (Figure 3C). Although low, this percentage is in agreement with the 11%–21% DC transfection using lipids⁶⁶ and with the 16% pluripotent stem cell transfection using RepRNA GFP.⁶⁷ No significant difference in transfection efficiency was observed at 24 h between LPPs and LFM (14% versus 18%, respectively). However, LFM yielded higher percentages of GFP-expressing cells at 48 h (27% versus 15% for LPPs) and 72 h (27% versus 16%). A low *in vitro* transfection efficiency of DCs does not imply an *in vivo* inefficiency. Indeed, lipidic nanoparticles prepared with luciferase RepRNA were not able to transfect DC 2.4 cells²⁹ but were capable of protective anti-influenza vaccination. This reflects the weak *in vitro/in vivo* correlation because of the increased complexity of the biological and physiological mechanisms at play in an animal model compared to a monolayer culture of a cell line.^{68,69} RepRNA expression in DC 2.4 cells after LPP transfection suggests an immunological role for LPP.

In Vivo Evaluation of LPP

The next set of experiments aimed to demonstrate the *in vivo* expression of RNA delivered using LPPs. To demonstrate the versatility of the LPP platform, we evaluated the delivery of both conventional mRNA and RepRNA (Figure 4). Conventional RNA was administered by an i.v. route to enhance accumulation of mRNA in the spleen and favor endocytosis of LPPs by splenic DCs, as in our previous studies^{14,15,70} and as in clinical studies (Heesch et al., 2016, Cancer Res., abstract).^{16,24} RepRNA was injected i.m. to allow localized amplification of RepRNA, rather than its dispersion after i.v. injection, and because most RepRNA vaccines have been injected i.m. in mice, macaques, and humans.^{22,29,36,71–73} Moreover, the i.m. route is a suitable route for the delivery of mRNA to lymph node DCs.⁷⁴

The evaluation of splenic DC transfection *in vivo* was performed 24 h and 48 h after i.v. injection of LPPs made with GFP mRNA. DCs were isolated from the spleen, and GFP expression was examined by flow cytometry (Figure 4A). LPP administration resulted in transfection of 5% at 24 h and 7% of splenic DCs at 48 h. Our data are in agreement with the 10% splenic DC transfection obtained with positively-charged mannosylated LPPs (+43 mV),^{7,15} the 5% GFP expressing splenic DCs after i.v. injection of positively-charged DOTAP lipoplexes (+27 mV),³⁸ and the 6% splenic DC transfection with negatively-charged lipoplexes (-20 mV).¹⁶ They are also similar to results on *in vivo* DC transfection using other administration routes with 5% inguinal lymph node DC transfection after subcutaneous injection of negatively charged (-10 mV) LNPs.³⁹

Table 2. Size and Zeta Potential of LPPs

DOPA/PEI (Molar Ratio)	Size (nm)	PDI	Zeta (mV)
18	186/10	0.13/0.02	2.5/1.4
23	190/8	0.13/0.01	0.5/0.2
25	188/9	0.14/0.07	1/0.9
32	157/16	0.12/0.02	1.1/0.5

RepRNA-LPPs were i.m. injected (5 µg RepRNA dose) before monitoring signal by luminescence imaging (Figures 4B and 4C). Durable luciferase expression was detectable at the site of injection from day 3 to day 14. The expression peaked at day 7 to day 10 before dropping at day 14 to the value at day 3. The delay observed in reporter gene expression together with a maximal expression at day 7 followed by a sharp signal decrease is in accordance with previous results of i.m. RepRNA delivery.^{29,36,71} The later onset of expression may be attributed to the delay necessary for expression of the replicase polyprotein, its cleavage to form the replicase complex, and amplification of RNA. The sharp decrease of expression detected can be attributed to the exhaustion and/or death of RepRNA-transfected cells.^{26,36} No signal was detected after injection of LFM-RepRNA complexes, albeit this transfection reagent is not intended for *in vivo* use (data not shown).

Immunogenicity of LPPs

Upon demonstration of *in vivo* expression, we explored the immunological potentiality of LPP-RepRNA complexes (Figure 5). Using adoptive transfer, we measured the induction of lymph node hemagglutinin (HA)-specific CD4 (Figure 5A) and CD8 (Figure 5B) cells. Induction of HA-specific T cells was also evaluated in the spleen (Figure 5C). Vaccination by i.m. route with LPP-RepRNA encoding HA resulted in the expansion of lymph node antigen-specific CD4⁺ T cells (3.5%) and CD8⁺ T cells (5.5%) as shown in Figures 5A and 5B. Administration of LPP-RepRNA also induced specific lymphocytes in the spleen, with a stimulation index superior to free RNA + adjuvant (Figure 5C). Lymphocytes induced by vaccination were functional, as evidenced by the 1.6-fold higher counts of antigen-specific CD4⁺ and CD8⁺ T cells secreting IFN-γ in the spleens of mice vaccinated with LPP-RepRNA over free RNA (Figure 5D). Induction of both CD4 and CD8 responses after RepRNA administration is consistent with previous data on i.m. vaccination with RepRNA lipidic nanoparticles.⁷¹

MATERIALS AND METHODS

All reagents were purchased from Sigma (St. Quentin Fallavier, France) unless otherwise stated. The mMESSAGING mMACHINE T7 ULTRA Transcription Kit, was purchased from Thermo Fisher Scientific (Montigny-le-Bretonneux, France). DOPE, DSPE-PEG, DOPA, and 16:0 PA-PEG3-mannose were from Avanti Polar Lipids (Alabaster, AL, USA).

Plasmids

The pGEM4Z-luc and pGEM4Z-EGFP plasmids used for the preparation of luciferase and EGFP RNA have been previously described.⁷

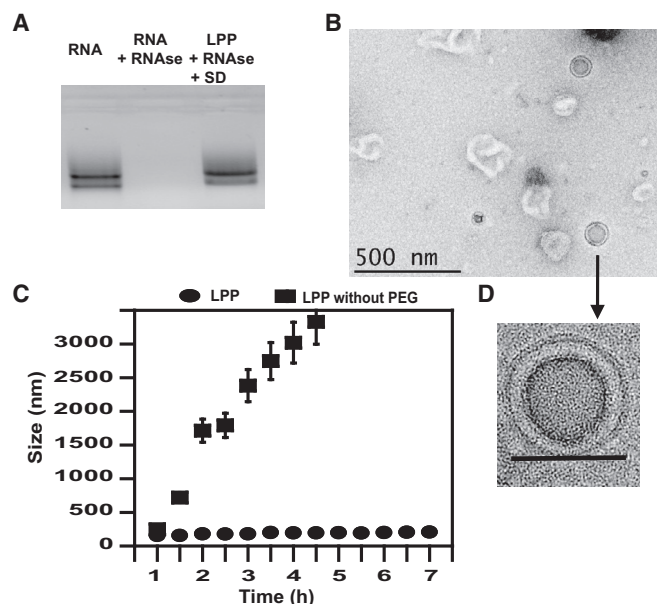


Figure 2. LPP Morphology and Stability

(A) RNase protection assay: lane 1, RNA; lane 2, RNA + RNase; lane 3, LPPs treated with RNase and dissociated with sulfated dextran (SD). (B) Morphology of LPPs by TEM at low magnification. Scale bar represents 500 nm. (C) Measurement of LPP diameters by DLS after incubation in media 10% FBS at 37°C. (D) Morphology of LPPs by TEM. Scale bar represents 100 nm.

The self-replicative RNA plasmid encoding GFP, pT7-VEE-GFP was a gift from Steven Dowdy (Addgene plasmid #58977). This plasmid is derived from Venezuelan equine encephalitis virus.⁷⁵ HA from influenza was synthesized by Genscript (Piscataway, NJ, USA) and inserted into previously digested pT7-VEE-GFP to replace GFP by HA to obtain pT7-VEE-HA. For the pT7-VEE-luc plasmid, we replaced the GFP of pT7-VEE-GFP with luc from pGEM4Z-luc. Plasmid DNA (pDNA) used in this study was amplified in *E. coli* DH5 α and purified using an Endofree Plasmid Mega Kit (QIAGEN, Courtabouef, France).

In Vitro Transcription

Anti-reverse cap analog (ARCA)-capped RNA with a poly(A) tail was produced by *in vitro* transcription using the T7 mMessage mMachine kit as described in Lin et al.⁶ and Perche et al.⁷ The RNA concentration was determined by absorbance at 260 nm; RNA had 260:280 ratios ≥ 2 and was stored at -80°C in endonuclease-free water in small aliquots.

Cell Culture

DC 2.4 murine DCs were a gift from Kenneth L. Rock⁷⁶ and were grown at 37°C in a humidified atmosphere containing 5% CO₂ in RPMI1640 medium supplemented with 10% heat-inactivated fetal bovine serum, 100 U/mL penicillin, and 100 μ g/mL streptomycin (Fischer Bioblock, Illkirch, France). Cells were mycoplasma-free, as evidenced by MycoAlert Mycoplasma Detection Kit (Lonza, Levallois Perret, France).

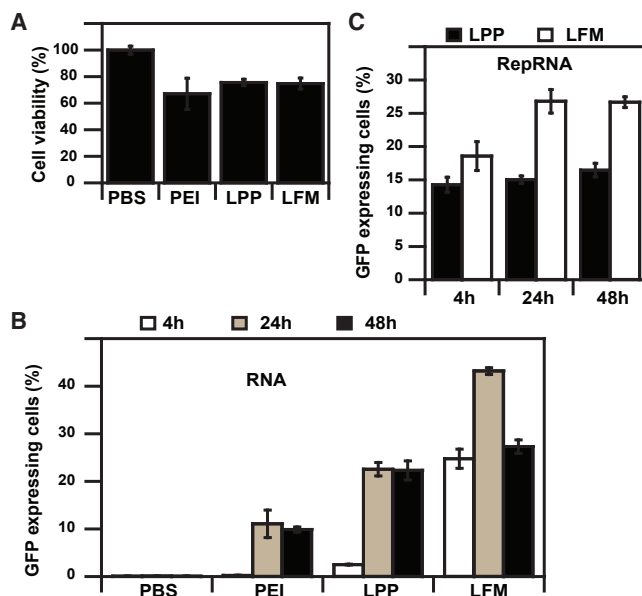


Figure 3. LPP Activity in Murine Dendritic Cells In Cellulo

(A) DC transfection efficiency of PEI, LPP, and LFM formulations made with 2 μ g GFP mRNA. (B) Cell viability of DCs 24 h after transfection with PEI 25K polyplexes, LPPs, or lipofectamine messenger max (LFM) complexes. (C) DC transfection efficiency of LPPs or LFM made with 2 μ g RepRNA.

Liposome Preparation

Liposomes were prepared by thin-film hydration as in Apte et al.⁷⁷ Both PEGylated and unPEGylated liposomes were prepared. A chloroform solution of 40% DOPA, 40% DOPE, 10% PA-PEG3-Man, and 10% DSPE-PEG2000 (molar percentages) was evaporated at 50°C in a rotary evaporator to form lipid films. Lipid films were hydrated with HEPES 10 mM pH 7.4 10% sucrose at a final lipid concentration of 5.4 mM. Liposomes were then sonicated for 15 min at 20°C at 37 kHz using an ultrasonic bath (Fischer Bioblock Scientific, Illkirch, France). Liposomes were then downsized by stepwise extrusion through 0.4 and 0.2 μ m pore-size filters using a mini-extruder from Avanti Polar Lipids.

Preparation of mRNA/PEI/Liposome LPPs

LPPs were prepared according to a procedure modified from Wang et al.⁶⁰ Instead of mixing polyplexes with a dried lipid film followed by sonication and extrusion, we mixed polyplexes with liposomes. To prepare LPPs, RNA was mixed with branched PEI of 25K in HEPES 10 mM pH 7.4 10% sucrose at an N/P ratio of 6 at room temperature for 20 min, allowing for polyplex formation. Note that PEI solution was added to RNA solution, as the order of addition is important for LPP formation.⁵¹ Then, different amounts of liposomes were added to polyplexes at DOPA/PEI molar ratios between 12 and 38.

LPP Characterization

The size and zeta potential of LPPs were determined by dynamic light scattering (DLS) using an SZ-100 nanoparticle analyzer (Horiba,

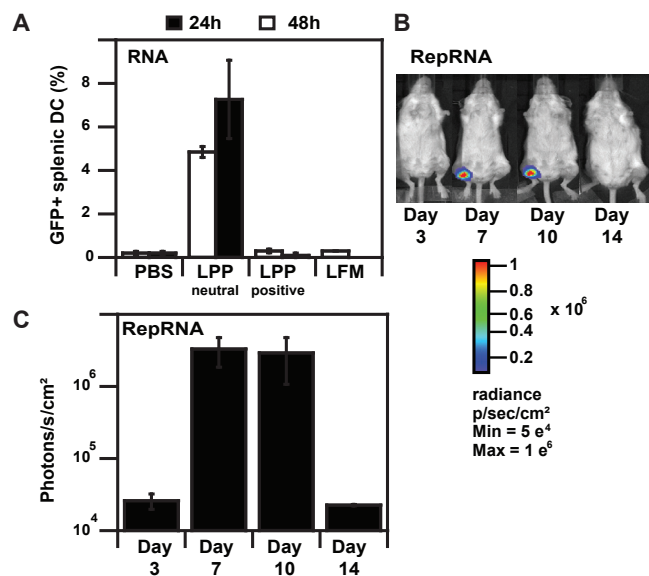


Figure 4. In Vivo RNA Expression after LPP-RNA Administration

(A) Percentages of murine splenic DC transfection after intravenous injection of LPP-RNA complexes (20 μg in 250 μL). (B) Bioluminescence imaging of BALB/c mice at various days following intramuscular injection of LPP-RepRNA complexes (5 μg in 50 μL); mean luminescence values are also shown in photons/seconds/ cm^2 .

Longjumeau, France). LPP structure was analyzed by transmission electron microscopy (TEM) using a Philips CM20/STEM electron microscope operating at 50 kV (Centre de Microscopie Electronique, Université d'Orléans, France). TEM samples were prepared according to the technique of negative staining using uranyl acetate. The basis of the method is to surround the light atoms sample with a dense stain to create TEM contrast. 5 μL LPP solution in HEPES buffer was deposited on a carbon-coated copper grid for 5 min and then adsorbed with filter paper. 5 μL uranyl acetate 2% in endonuclease-free water was then deposited on the grid for 10 s and then adsorbed. Samples were dried at room temperature for 20 min before TEM observation.

The concentration of mannosylated lipids in liposomes was estimated by a resorcinol/sulfuric acid assay as described in Perche et al.⁷ The principle is that, under acidic conditions, sugars dehydrate, forming a furfural derivative, which condenses with resorcinol to yield a chromogenic compound with an absorbance at 430 nm. Briefly, samples or standards are deposited into 96-well microplates before successive addition of a resorcinol solution in water and a solution of 75% sulfuric acid. The plate is then heated at 90°C during 30 min before reading the absorbance at 430 nm.

RNase Protection Assay

RNase protection assay was performed according to Perche et al.⁷⁸ Samples containing 2 μg mRNA were incubated with 5 U of RNase A/T1 Mix (Thermo scientific) for 2 h at 37°C. The RNase was then inactivated with Protector RNase Inhibitor (Roche) before complex dissociation using sulfated dextran (10% of final volume). Then, sam-

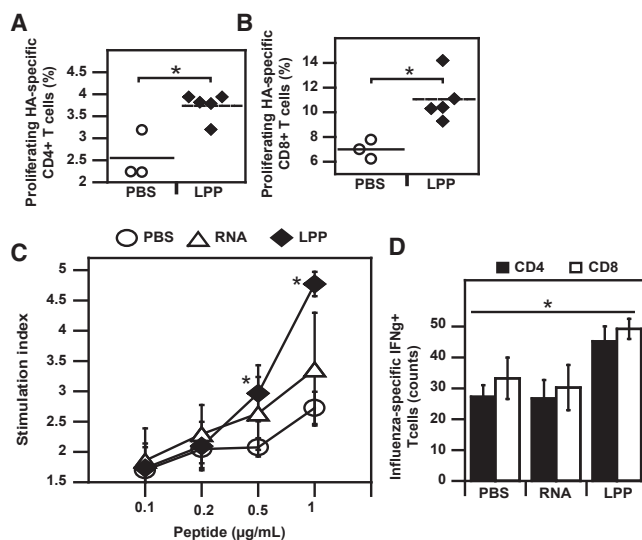


Figure 5. Immunogenicity of LPP-RepRNA

(A and B) Mice were vaccinated by intramuscular injection of LPP-RepRNA. We analyzed the induction of HA-specific T cells in the lymph nodes, both CD4 (A) and CD8 (B). Stimulation indexes of splenocytes from vaccinated mice after re-stimulation with HA peptide (C) and counts of IFN- γ secreting splenic T cells. ** $p < 0.01$ compared with RepRNA.

ples were analyzed on a 1% agarose-formaldehyde gel containing ethidium bromide. Gels were imaged using a Gene Flash imager (Syngene, Cambridge, UK).

Transfections

Cells were transfected with either LPP or LFM (Thermo Fisher Scientific) as commercial standard at 70%–80% confluency in 24-well plates containing 2 μg RNA encoding GFP per well. Transfection efficiency was evaluated at 4 h, 24 h, or 48 h after transfection. The cell-associated fluorescence intensity was measured with a flow cytometer (FACSsort; Becton Dickinson, Franklin Lakes, NJ, USA) with $\lambda_{\text{ex}} = 488 \text{ nm}$; $\lambda_{\text{em}} = 530 \pm 30 \text{ nm}$. The fluorescence intensity was expressed as the mean fluorescence intensity of 10,000 events.

In Vitro Cytotoxicity

Cytotoxicity was evaluated performing an MTT (3-(4,5-dimethylthiazol-2-yl)-2,5-diphenyltetrazolium bromide) assay as described in Perche et al.⁷⁰ This assay is based on the reduction of soluble MTT into insoluble formazan (with absorbance at 570 nm) by cellular oxidoreductases. MTT (200 μL of a 5 mg/mL solution in PBS) was added to the cells in 1 mL culture medium, and cells were incubated for 3 h at 37°C. Cells were then washed with PBS, and the MTT converted in formazan was solubilized with acidic isopropanol (99.5%). The cell viability was expressed as a percentage of absorbance of untransfected cells cultured in the same conditions.

In Vivo Evaluation of Splenic DC Transfection

Specific pathogen-free female BALB/c (8–11 weeks) mice were obtained from Janvier (Le Genest St Isle, France) and kept in isolated

ventilated cages. All animal studies were approved by the French Ministry of Agriculture for experiments with laboratory animals.

Mice received 20 μg EGFP mRNA/LPP in HEPES 5% sucrose by i.v. injection in the tail vein (volume of 250 μL). Control mice received 250 μL HEPES 5% sucrose. Evaluation of splenic DC transfection was carried out as described in Perche et al.⁷ Spleens were harvested 24 h or 48 h after injection. Splenic cells were isolated and labeled with magnetic anti-mouse CD11c antibodies (Miltenyi Biotec SAS, Paris, France), which bound to DCs and were enriched by immunomagnetic selection using MACS MS columns (Miltenyi Biotec SAS) according to the manufacturer's protocol. Then, cells were stained with BV711-labeled anti-mouse CD11c antibodies (Miltenyi Biotec SAS), and at least 40,000 cells were analyzed with a FORTRESSA X20 flow cytometer (Becton Dickinson) with $\lambda_{\text{ex}} = 488 \text{ nm}$, $\lambda_{\text{em}} = 530/30 \text{ nm}$ for EGFP fluorescence and $\lambda_{\text{ex}} = 405 \text{ nm}$, $\lambda_{\text{em}} = 710/50 \text{ nm}$ for BV711 fluorescence. BV711 is a Horizon Brilliant Violet tandem fluorophore (Beckton Dickinson) of BD Horizon BV421 with a maximum λ_{ex} at 405 nm and an acceptor dye with a maximum λ_{em} at 711 nm.

Measurement of *In Vivo* Luminescence

Mice were i.m.-injected with LPPs prepared with 5 μg RepRNA encoding luciferase (50 μL injection volume). Animals were imaged as described in Lin et al.⁶ using an IVIS Lumina system imaging system (PerkinElmer, Villebon-sur-Yvette, France) 5 min after intraperitoneal injection of 200 μL D-Luciferin substrate at the CIPA (Centre d'Imagerie du Petit Animal, Orléans, France).

Animals for Functional Evaluation

Six- to eight-week-old female BALB/c mice were purchased either from Harlan Winkelmann (Germany) or Janvier Labs (France) and maintained in the animal care facility of the Helmholtz Centre for Infection Research. All animal experiments were approved by the Helmholtz-Zentrum für Infektionsforschung (HZI) ethical board and conducted in accordance with the regulations of the local government of Lower Saxony (Germany, 33-42502-04-13/1281 and 33-42502-04-16/2118).

Adoptive Transfer

For the adoptive transfer experiments, T cell receptor (TCR)-HA transgenic mice were used as described in Englezou et al.²³ Briefly, the proliferation of antigen-specific CFSE-labeled (carboxyfluorescein succinimidyl ester) T cells derived from TCR-HA mice were transferred by i.v. injection to naive BALB/c mice. Then, mice were vaccinated 24 h after injection of the CFSE-labeled splenocytes with LPPs prepared with HA RepRNA co-administered with c-di-AMP adjuvant. Proliferation, via loss of CFSE staining of CD4⁺ and CD8⁺ T cells, was determined by flow cytometry.

Immunization

Mice were immunized three times with 10 μg HA RepRNA/LPPs co-administered with c-di-AMP (10 μg) by i.m. route (50 μL injection volume), with one immunization (day 0) and two boosts (days 21

and 42). Two weeks later, spleens of vaccinated mice were aseptically removed, cell suspensions using pools of spleen cells of different immunized groups were prepared, and erythrocytes were lysed by a short-term incubation (maximum of 2 min) in ACK lysis buffer (0.15 M NH_4Cl , 1.0 M KHCO_3 , 0.1 mM EDTA, pH 7.2). Then cells were washed twice and adjusted to 2×10^6 cells/mL in complete RPMI medium (containing 10% fetal bovine serum, 100 U/mL penicillin, and 100 $\mu\text{g}/\text{mL}$ streptomycin; GIBCO, UK). Then splenocytes (2×10^7 cells/mL) were incubated (37°C , 5% CO_2) in RPMI containing the HA antigen (#13/164, 200 ng HA/mL) or no antigen to determine the basal cytokine production. Viable singlet leukocytes were gated for CD3, CD4, and CD8 and subsequently analyzed for the expression of intracellular IFN- γ .

Measurement of Cellular Proliferation

To study T cell polarization, we used CD4 and CD8 T cells from TCR-HA mice. These mice express rearranged TCR α/β chains specific for the MHC class II I-E_d restricted determinant site from influenza virus A/PR/8/34 HA (PR8 HA).³⁷ *In vitro*-enriched CD4⁺ and CD8⁺ T cells from TCR-HA transgenic animals were adoptively transferred to normal BALB/c mice. Recipient mice received $2\text{--}3 \times 10^6$ CFSE-labeled cells by tail vein injection and were immunized by i.m. injection of 50 μL of 10 μg HA RepRNA/LPP co-administered with c-di-AMP (10 μg). After 7 days, the mice were sacrificed, and spleens and draining inguinal or cervical lymph nodes (LNs) were aseptically removed. Lymph nodes were filtered through a mesh to get a single suspension. After two wash steps with PBS (centrifugation with $200 \times g/5 \text{ min}$), lymph node cells were ready to be used for subsequent FACS analysis or CFSE staining. The splenocyte pools of each group were cultured in the presence of different concentrations of H1N1 (#13/164) with enhanced HA concentrations of 0.1 up to 1 $\mu\text{g}/\text{mL}$; controls received 5 $\mu\text{g}/\text{mL}$ concanavalin A as described in Ebensen et al.⁷⁹ After staining for CD3, CD4, CD8, CD19, and the live/dead marker (LIVE/DEAD Fixable Dead Cell Stain Kit from Invitrogen) as a marker of viability, cells were fixated with 2% paraformaldehyde (PFA). Readout was performed by flow cytometry.

Multifunctional T Cells

Splenocytes (2×10^7 cells/mL) were incubated (37°C , 5% CO_2) in RPMI containing the HA antigen (H1N1, 200 ng HA/mL) or no antigen to determine the basal cytokine production. Viable singlet leukocytes were gated for CD3⁺ CD4⁺ or CD3⁺ CD8⁺ and subsequently analyzed for the expression of intracellular IFN- γ by flow cytometry as described in Ebensen et al.⁷⁹

Statistical Analysis

The data were tested for statistical significance using ANOVA. All numerical data are expressed as mean \pm SD, $n = 3$. Any p value less than 0.05 was considered statistically significant.

Conclusions

The results of this study are, to the best of our knowledge, the first on conventional and self-replicative RNA expression *in vivo* using the same formulation. LPPs are stable in serum-containing media,

transfect DCs *in cellulo* and their injection results in reporter gene expression *in vivo* and, to the induction of antigen-specific immune responses. Our data on conventional RNA delivery as LPP-RNA complexes corroborates the reported splenic DC transfection after i.v. administration of negative-to-neutral lipoplexes.^{16,80} Moreover, i.m. injection of LPP-RepRNA complexes led to sustained reporter gene expression *in vivo* and the induction of functional antigen-specific T cells when LPP-RepRNA coded for an influenza antigen.

Taken together, our strategy has the potential for the delivery of both conventional and self-replicative RNA, providing a platform for various therapeutic applications. Determination of the therapeutic activity of i.v. injected LPP-RNA complexes and locally injected LPP-RepRNA complexes will be our prime focus in the future.

AUTHOR CONTRIBUTIONS

F.P. and C.P. conceived the idea. F.P., R.C., T.E., and K.S. performed the experiments. F.P., T.E., K.S., C.P., and C.A.G. analyzed data. All authors wrote the manuscript.

CONFLICTS OF INTEREST

CAG and TE are inventors in patents covering the use of c-di-AMP as adjuvant (PCT/EP 2006010693, EP/04.04.02/EPA 02007640 and, PCT/EP2006011182). This does not alter the authors' adherence to the policy of sharing data and materials.

ACKNOWLEDGMENTS

We are grateful to Dr. Bertrand Castaing for providing access to the Nano S zetasiser. We also thank Audrey Sauldubois from the Centre de Microscopie Electronique platform (Université d'Orléans) for TEM studies. This work was supported by the EU FP7 Project UNIVAX (HEALTH-F3-2013-60173).

REFERENCES

- Sahin, U., Karikó, K., and Türeci, Ö. (2014). mRNA-based therapeutics—developing a new class of drugs. *Nat. Rev. Drug Discov.* *13*, 759–780.
- Zangi, L., Lui, K.O., von Gise, A., Ma, Q., Ebina, W., Ptaszek, L.M., Später, D., Xu, H., Tabebordbar, M., Gorbатов, R., et al. (2013). Modified mRNA directs the fate of heart progenitor cells and induces vascular regeneration after myocardial infarction. *Nat. Biotechnol.* *31*, 898–907.
- Kaczmarek, J.C., Kowalski, P.S., and Anderson, D.G. (2017). Advances in the delivery of RNA therapeutics: from concept to clinical reality. *Genome Med.* *9*, 60.
- Zou, S., Scarfo, K., Nantz, M.H., and Hecker, J.G. (2010). Lipid-mediated delivery of RNA is more efficient than delivery of DNA in non-dividing cells. *Int. J. Pharm.* *389*, 232–243.
- Perche, F., Uchida, S., Akiba, H., Lin, C.-Y., Ikegami, M., Dirisala, A., Nakashima, T., Itaka, K., Tsumoto, K., and Kataoka, K. (2017). Improved brain expression of anti-amyloid β scfv by complexation of mRNA including a secretion sequence with PEG-based block cationer. *Curr. Alzheimer Res.* *14*, 295–302.
- Lin, C.-Y., Perche, F., Ikegami, M., Uchida, S., Kataoka, K., and Itaka, K. (2016). Messenger RNA-based therapeutics for brain diseases: An animal study for augmenting clearance of beta-amyloid by intracerebral administration of neprilysin mRNA loaded in polyplex nanomicelles. *J. Control. Release* *235*, 268–275.
- Perche, F., Benvegna, T., Berchel, M., Lebegue, L., Pichon, C., Jaffrès, P.-A., and Midoux, P. (2011). Enhancement of dendritic cells transfection *in vivo* and of vaccination against B16F10 melanoma with mannoseylated histidylated lipopolyplexes loaded with tumor antigen messenger RNA. *Nanomedicine (Lond.)* *7*, 445–453.
- Kirschman, J.L., Bhosle, S., Vanover, D., Blanchard, E.L., Loomis, K.H., Zurla, C., Murray, K., Lam, B.C., and Santangelo, P.J. (2017). Characterizing exogenous mRNA delivery, trafficking, cytoplasmic release and RNA-protein correlations at the level of single cells. *Nucleic Acids Res.* *45*, e113.
- Diken, M., Kreiter, S., Selmi, A., Britten, C.M., Huber, C., Türeci, Ö., and Sahin, U. (2011). Selective uptake of naked vaccine RNA by dendritic cells is driven by macropinocytosis and abrogated upon DC maturation. *Gene Ther.* *18*, 702–708.
- Kreiter, S., Selmi, A., Diken, M., Koslowski, M., Britten, C.M., Huber, C., Türeci, Ö., and Sahin, U. (2010). Intranasal vaccination with naked antigen-encoding RNA elicits potent prophylactic and therapeutic antitumoral immunity. *Cancer Res.* *70*, 9031–9040.
- Van Lint, S., Goyvaerts, C., Maenhout, S., Goethals, L., Disy, A., Benteyn, D., Pen, J., Bonehill, A., Heirman, C., Breckpot, K., and Thielemans, K. (2012). Preclinical evaluation of TriMix and antigen mRNA-based antitumor therapy. *Cancer Res.* *72*, 1661–1671.
- Shortman, K., and Liu, Y.-J. (2002). Mouse and human dendritic cell subtypes. *Nat. Rev. Immunol.* *2*, 151–161.
- Goyvaerts, C., and Breckpot, K. (2015). Pros and cons of antigen-presenting cell targeted tumor vaccines. *J. Immunol. Res.* *2015*, 785634.
- Le Moignic, A., Malard, V., Benvegna, T., Lemiègre, L., Berchel, M., Jaffrès, P.-A., Baillou, C., Delost, M., Macedo, R., Rochefort, J., et al. (2018). Preclinical evaluation of mRNA trimannosylated lipopolyplexes as therapeutic cancer vaccines targeting dendritic cells. *J. Control. Release* *278*, 110–121.
- Van der Jeught, K., De Koker, S., Bialkowski, L., Heirman, C., Tjok Joe, P., Perche, F., Maenhout, S., Bevers, S., Broos, K., Deswarte, K., et al. (2018). Dendritic Cell Targeting mRNA Lipopolyplexes Combine Strong Antitumor T-Cell Immunity with Improved Inflammatory Safety. *ACS Nano* *12*, 9815–9829.
- Kranz, L.M., Diken, M., Haas, H., Kreiter, S., Loquai, C., Reuter, K.C., Meng, M., Fritz, D., Vascotto, F., Hefesha, H., et al. (2016). Systemic RNA delivery to dendritic cells exploits antiviral defence for cancer immunotherapy. *Nature* *534*, 396–401.
- Schädlich, A., Caysa, H., Mueller, T., Tenambergen, F., Rose, C., Göpferich, A., Kuntsche, J., and Mäder, K. (2011). Tumor accumulation of NIR fluorescent PEG-PLA nanoparticles: impact of particle size and human xenograft tumor model. *ACS Nano* *5*, 8710–8720.
- Mebius, R.E., and Kraal, G. (2005). Structure and function of the spleen. *Nat. Rev. Immunol.* *5*, 606–616.
- Bae, Y.H., and Park, K. (2011). Targeted drug delivery to tumors: myths, reality and possibility. *J. Control. Release* *153*, 198–205.
- Gustafson, H.H., Holt-Casper, D., Grainger, D.W., and Ghandehari, H. (2015). Nanoparticle uptake: the phagocyte problem. *Nano Today* *10*, 487–510.
- Pardi, N., Hogan, M.J., Pelc, R.S., Muramatsu, H., Andersen, H., DeMaso, C.R., Dowd, K.A., Sutherland, L.L., Scarce, R.M., Parks, R., et al. (2017). Zika virus protection by a single low-dose nucleoside-modified mRNA vaccination. *Nature* *543*, 248–251.
- Bahl, K., Senn, J.J., Yuzhakov, O., Bulychev, A., Brito, L.A., Hassett, K.J., Laska, M.E., Smith, M., Almarsson, Ö., Thompson, J., et al. (2017). Preclinical and clinical demonstration of immunogenicity by mRNA vaccines against H10N8 and H7N9 influenza viruses. *Mol. Ther.* *25*, 1316–1327.
- Englezou, P.C., Sapet, C., Démoulin, T., Milona, P., Ebensen, T., Schulze, K., Guzman, C.A., Poulhes, F., Zelphati, O., Ruggli, N., and McCullough, K.C. (2018). Self-Amplifying Replicon RNA Delivery to Dendritic Cells by Cationic Lipids. *Mol. Ther. Nucleic Acids* *12*, 118–134.
- Jabulowsky, R.A., Loquai, C., Diken, M., Kranz, L.M., Haas, H., Attig, S., et al. (2016). Abstract CT032: a first-in-human phase I/II clinical trial assessing novel mRNA-lipoplex nanoparticles for potent cancer immunotherapy in patients with malignant melanoma (AACR).
- Midoux, P., and Pichon, C. (2015). Lipid-based mRNA vaccine delivery systems. *Expert Rev. Vaccines* *14*, 221–234.
- Ying, H., Zaks, T.Z., Wang, R.-F., Irvine, K.R., Kammula, U.S., Marincola, F.M., Leitner, W.W., and Restifo, N.P. (1999). Cancer therapy using a self-replicating RNA vaccine. *Nat. Med.* *5*, 823–827.
- Barbeau, J., Lemiègre, L., Quelen, A., Malard, V., Gao, H., Gonçalves, C., Berchel, M., Jaffrès, P.A., Pichon, C., Midoux, P., and Benvegna, T. (2016). Synthesis of a

- trimannosylated-equipped archaeal diether lipid for the development of novel glycoliposomes. *Carbohydr. Res.* *435*, 142–148.
28. Scorza, F.B., and Pardi, N. (2018). New kids on the block: RNA-based influenza virus vaccines. *Vaccines (Basel)* *6*, 20.
 29. Chahal, J.S., Khan, O.F., Cooper, C.L., McPartlan, J.S., Tsosie, J.K., Tilley, L.D., Sidik, S.M., Lourido, S., Langer, R., Bavari, S., et al. (2016). Dendrimer-RNA nanoparticles generate protective immunity against lethal Ebola, H1N1 influenza, and *Toxoplasma gondii* challenges with a single dose. *Proc. Natl. Acad. Sci. USA* *113*, E4133–E4142.
 30. Ljungberg, K., and Liljeström, P. (2015). Self-replicating alphavirus RNA vaccines. *Expert Rev. Vaccines* *14*, 177–194.
 31. McCullough, K.C., Bassi, I., Démoulin, T., Thomann-Harwood, L.J., and Ruggli, N. (2012). Functional RNA delivery targeted to dendritic cells by synthetic nanoparticles. *Ther. Deliv.* *3*, 1077–1099.
 32. Wei, C.-J., Boyington, J.C., McTamney, P.M., Kong, W.-P., Pearce, M.B., Xu, L., Andersen, H., Rao, S., Tumpey, T.M., Yang, Z.Y., and Nabel, G.J. (2010). Induction of broadly neutralizing H1N1 influenza antibodies by vaccination. *Science* *329*, 1060–1064.
 33. Price, G.E., Soboleski, M.R., Lo, C.-Y., Misplon, J.A., Quirion, M.R., Houser, K.V., Pearce, M.B., Pappas, C., Tumpey, T.M., and Epstein, S.L. (2010). Single-dose mucosal immunization with a candidate universal influenza vaccine provides rapid protection from virulent H5N1, H3N2 and H1N1 viruses. *PLoS ONE* *5*, e13162.
 34. Poon, L.L., Leung, Y.H., Nicholls, J.M., Perera, P.-Y., Lichy, J.H., Yamamoto, M., Waldmann, T.A., Peiris, J.S., and Perera, L.P. (2009). Vaccinia virus-based multivalent H5N1 avian influenza vaccines adjuvanted with IL-15 confer sterile cross-clade protection in mice. *J. Immunol.* *182*, 3063–3071.
 35. Zhou, D., Wu, T.-L., Lasaro, M.O., Latimer, B.P., Parzych, E.M., Bian, A., Li, Y., Li, H., Erikson, J., Xiang, Z., and Ertl, H.C. (2010). A universal influenza A vaccine based on adenovirus expressing matrix-2 ectodomain and nucleoprotein protects mice from lethal challenge. *Mol. Ther.* *18*, 2182–2189.
 36. Vogel, A.B., Lambert, L., Kinnear, E., Busse, D., Erbar, S., Reuter, K.C., Wicke, L., Perkovic, M., Beissert, T., Haas, H., et al. (2018). Self-Amplifying RNA Vaccines Give Equivalent Protection against Influenza to mRNA Vaccines but at Much Lower Doses. *Mol. Ther.* *26*, 446–455.
 37. Ulmer, J.B., and Geall, A.J. (2016). Recent innovations in mRNA vaccines. *Curr. Opin. Immunol.* *41*, 18–22.
 38. Sayour, E.J., De Leon, G., Pham, C., Grippin, A., Kemeny, H., Chua, J., Huang, J., Sampson, J.H., Sanchez-Perez, L., Flores, C., and Mitchell, D.A. (2016). Systemic activation of antigen-presenting cells via RNA-loaded nanoparticles. *Oncolimmunology* *6*, e1256527.
 39. Oberli, M.A., Reichmuth, A.M., Dorkin, J.R., Mitchell, M.J., Fenton, O.S., Jaklenec, A., Anderson, D.G., Langer, R., and Blankschtein, D. (2017). Lipid nanoparticle assisted mRNA delivery for potent cancer immunotherapy. *Nano Lett.* *17*, 1326–1335.
 40. Ranneh, A.H., Takemoto, H., Sakuma, S., Awaad, A., Nomoto, T., Mochida, Y., Matsui, M., Tomoda, K., Naito, M., and Nishiyama, N. (2018). An Ethylenediamine-based Switch to Render the Polyzwitterion Cationic at Tumorous pH for Effective Tumor Accumulation of Coated Nanomaterials. *Angew. Chem. Int. Ed. Engl.* *57*, 5057–5061.
 41. Yuan, Y.Y., Mao, C.Q., Du, X.J., Du, J.Z., Wang, F., and Wang, J. (2012). Surface charge switchable nanoparticles based on zwitterionic polymer for enhanced drug delivery to tumor. *Adv. Mater.* *24*, 5476–5480.
 42. Chen, L., Simpson, J.D., Fuchs, A.V., Rolfe, B.E., and Thurecht, K.J. (2017). Effects of surface charge of hyperbranched polymers on cytotoxicity, dynamic cellular uptake and localization, hemotoxicity, and pharmacokinetics in mice. *Mol. Pharm.* *14*, 4485–4497.
 43. Xia, Y., Tian, J., and Chen, X. (2016). Effect of surface properties on liposomal siRNA delivery. *Biomaterials* *79*, 56–68.
 44. Meng, H., Leong, W., Leong, K.W., Chen, C., and Zhao, Y. (2018). Walking the line: The fate of nanomaterials at biological barriers. *Biomaterials* *174*, 41–53.
 45. Chonn, A., Cullis, P.R., and Devine, D.V. (1991). The role of surface charge in the activation of the classical and alternative pathways of complement by liposomes. *J. Immunol.* *146*, 4234–4241.
 46. Harris, J.M., and Chess, R.B. (2003). Effect of pegylation on pharmaceuticals. *Nat. Rev. Drug Discov.* *2*, 214–221.
 47. Nance, E.A., Woodworth, G.F., Sailor, K.A., Shih, T.-Y., Xu, Q., Swaminathan, G., Xiang, D., Eberhart, C., and Hanes, J. (2012). A dense poly (ethylene glycol) coating improves penetration of large polymeric nanoparticles within brain tissue. *Sci. Transl. Med.* *4*, 149ra119.
 48. Trevasakis, N.L., Kaminskas, L.M., and Porter, C.J. (2015). From sewer to saviour - targeting the lymphatic system to promote drug exposure and activity. *Nat. Rev. Drug Discov.* *14*, 781–803.
 49. Jiang, H., Wang, Q., and Sun, X. (2017). Lymph node targeting strategies to improve vaccination efficacy. *J. Control. Release* *267*, 47–56.
 50. Rezaee, M., Oskuee, R.K., Nassirli, H., and Malaekheh-Nikouei, B. (2016). Progress in the development of lipopolyplexes as efficient non-viral gene delivery systems. *J. Control. Release* *236*, 1–14.
 51. Tros de Ilarduya, C., García, L., and Düzgünes, N. (2010). Liposomes and lipopolymeric carriers for gene delivery. *J. Microencapsul.* *27*, 602–608.
 52. García, L., Buñuales, M., Düzgünes, N., and Tros de Ilarduya, C. (2007). Serum-resistant lipopolyplexes for gene delivery to liver tumour cells. *Eur. J. Pharm. Biopharm.* *67*, 58–66.
 53. Uzgün, S., Nica, G., Pfeifer, C., Bosinco, M., Michaelis, K., Lutz, J.-F., Schneider, M., Rosenecker, J., and Rudolph, C. (2011). PEGylation improves nanoparticle formation and transfection efficiency of messenger RNA. *Pharm. Res.* *28*, 2223–2232.
 54. Perche, F., and Torchilin, V.P. (2013). Recent trends in multifunctional liposomal nanocarriers for enhanced tumor targeting. *J. Drug Deliv.* *2013*, 705265.
 55. Goodwin, T.J., and Huang, L. (2017). Investigation of phosphorylated adjuvants co-encapsulated with a model cancer peptide antigen for the treatment of colorectal cancer and liver metastasis. *Vaccine* *35*, 2550–2557.
 56. Yanasarn, N., Sloat, B.R., and Cui, Z. (2011). Negatively charged liposomes show potent adjuvant activity when simply admixed with protein antigens. *Mol. Pharm.* *8*, 1174–1185.
 57. Farhood, H., Serbina, N., and Huang, L. (1995). The role of dioleoyl phosphatidylethanolamine in cationic liposome mediated gene transfer. *Biochim. Biophys. Acta* *1235*, 289–295.
 58. Lee, C.-M., Choi, Y., Huh, E.J., Lee, K.Y., Song, H.-C., Sun, M.J., Jeong, H.J., Cho, C.S., and Bom, H.S. (2005). Polyethylene glycol (PEG) modified 99mTc-HMPAO-liposome for improving blood circulation and biodistribution: the effect of the extent of PEGylation. *Cancer Biother. Radiopharm.* *20*, 620–628.
 59. Buyens, K., De Smedt, S.C., Braeckmans, K., Demeester, J., Peeters, L., van Grunsven, L.A., de Mollerat du Jeu, X., Sawant, R., Torchilin, V., Farkasova, K., et al. (2012). Liposome based systems for systemic siRNA delivery: stability in blood sets the requirements for optimal carrier design. *J. Control. Release* *158*, 362–370.
 60. Wang, L.-L., Feng, C.-L., Zheng, W.-S., Huang, S., Zhang, W.-X., Wu, H.-N., Zhan, Y., Han, Y.X., Wu, S., and Jiang, J.D. (2017). Tumor-selective lipopolyplex encapsulated small active RNA hampers colorectal cancer growth in vitro and in orthotopic murine. *Biomaterials* *141*, 13–28.
 61. Pinnapireddy, S.R., Duse, L., Strehlow, B., Schäfer, J., and Bakowsky, U. (2017). Composite liposome-PEI/nucleic acid lipopolyplexes for safe and efficient gene delivery and gene knockdown. *Colloids Surf. B Biointerfaces* *158*, 93–101.
 62. Persano, S., Guevara, M.L., Li, Z., Mai, J., Ferrari, M., Pompa, P.P., and Shen, H. (2017). Lipopolyplex potentiates anti-tumor immunity of mRNA-based vaccination. *Biomaterials* *125*, 81–89.
 63. Zhao, W., Zhuang, S., and Qi, X.R. (2011). Comparative study of the in vitro and in vivo characteristics of cationic and neutral liposomes. *Int. J. Nanomedicine* *6*, 3087–3098.
 64. Nowakowski, A., Andrzejewska, A., Boltze, J., Nitzsche, F., Cui, L.L., Jolkonen, J., Walczak, P., Lukomska, B., and Janowski, M. (2017). Translation, but not transfection limits clinically relevant, exogenous mRNA based induction of alpha-4 integrin expression on human mesenchymal stem cells. *Sci. Rep.* *7*, 1103.
 65. Hajj, K.A., Ball, R.L., Deluty, S.B., Singh, S.R., Strelkova, D., Knapp, C.M., and Whitehead, K.A. (2019). Branched-Tail Lipid Nanoparticles Potently Deliver mRNA In Vivo due to Enhanced Ionization at Endosomal pH. *Small* *15*, e1805097.
 66. McCullough, K.C., Milona, P., Thomann-Harwood, L., Démoulin, T., Englezou, P., Suter, R., and Ruggli, N. (2014). Self-amplifying replicon RNA vaccine delivery to dendritic cells by synthetic nanoparticles. *Vaccines (Basel)* *2*, 735–754.

67. Yoshioka, N., and Dowdy, S.F. (2017). Enhanced generation of iPSCs from older adult human cells by a synthetic five-factor self-replicative RNA. *PLoS ONE* *12*, e0182018.
68. Paunovska, K., Sago, C.D., Monaco, C.M., Hudson, W.H., Castro, M.G., Rudoltz, T.G., Kalathoor, S., Vanover, D.A., Santangelo, P.J., Ahmed, R., et al. (2018). A direct comparison of in vitro and in vivo nucleic acid delivery mediated by hundreds of nanoparticles reveals a weak correlation. *Nano Lett.* *18*, 2148–2157.
69. Buck, J., Grossen, P., Cullis, P.R., Huwyler, J., and Witzigmann, D. (2019). Lipid-Based DNA Therapeutics: Hallmarks of Non-Viral Gene Delivery. *ACS Nano* *13*, 3754–3782.
70. Perche, F., Gosset, D., Mével, M., Miramon, M.-L., Yaouanc, J.-J., Pichon, C., Benvegno, T., Jaffrès, P.A., and Midoux, P. (2011). Selective gene delivery in dendritic cells with mannosylated and histidylated lipopolyplexes. *J. Drug Target.* *19*, 315–325.
71. Pepini, T., Pulichino, A.-M., Carsillo, T., Carlson, A.L., Sari-Sarraf, F., Ramsauer, K., Debasitis, J.C., Maruggi, G., Otten, G.R., Geall, A.J., et al. (2017). Induction of an IFN-mediated antiviral response by a self-amplifying RNA vaccine: implications for vaccine design. *J. Immunol.* *198*, 4012–4024.
72. Magini, D., Giovani, C., Mangiavacchi, S., Maccari, S., Cecchi, R., Ulmer, J.B., De Gregorio, E., Geall, A.J., Brazzoli, M., and Bertholet, S. (2016). Self-amplifying mRNA vaccines expressing multiple conserved influenza antigens confer protection against homologous and heterosubtypic viral challenge. *PLoS ONE* *11*, e0161193.
73. Brito, L.A., Chan, M., Shaw, C.A., Hekele, A., Carsillo, T., Schaefer, M., Archer, J., Seubert, A., Otten, G.R., Beard, C.W., et al. (2014). A cationic nanoemulsion for the delivery of next-generation RNA vaccines. *Mol. Ther.* *22*, 2118–2129.
74. Lindsay, K.E., Bhosle, S.M., Zurla, C., Beyersdorf, J., Rogers, K.A., Vanover, D., Xiao, P., Araínga, M., Shirreff, L.M., Pitard, B., et al. (2019). Visualization of early events in mRNA vaccine delivery in non-human primates via PET-CT and near-infrared imaging. *Nat. Biomed. Eng.* *3*, 371–380.
75. Yoshioka, N., Gros, E., Li, H.-R., Kumar, S., Deacon, D.C., Maron, C., Muotri, A.R., Chi, N.C., Fu, X.D., Yu, B.D., and Dowdy, S.F. (2013). Efficient generation of human iPSCs by a synthetic self-replicative RNA. *Cell Stem Cell* *13*, 246–254.
76. Shen, Z., Reznikoff, G., Dranoff, G., and Rock, K.L. (1997). Cloned dendritic cells can present exogenous antigens on both MHC class I and class II molecules. *J. Immunol.* *158*, 2723–2730.
77. Apte, A., Koren, E., Koshkaryev, A., and Torchilin, V.P. (2014). Doxorubicin in TAT peptide-modified multifunctional immunoliposomes demonstrates increased activity against both drug-sensitive and drug-resistant ovarian cancer models. *Cancer Biol. Ther.* *15*, 69–80.
78. Perche, F., Biswas, S., Patel, N.R., and Torchilin, V.P. (2016). Hypoxia-responsive copolymer for siRNA delivery. *Methods Mol. Biol.* *1372*, 139–162.
79. Ebensen, T., Debarry, J., Pedersen, G.K., Blazejewska, P., Weissmann, S., Schulze, K., McCullough, K.C., Cox, R.J., and Guzmán, C.A. (2017). Mucosal administration of cycle-di-nucleotide-adjuvanted virosomes efficiently induces protection against influenza H5N1 in mice. *Front. Immunol.* *8*, 1223.
80. Romani, B., Kavyanifard, A., and Allahbakhshi, E. (2017). Antibody production by in vivo RNA transfection. *Sci. Rep.* *7*, 10863.